

# HIGH-ORDER ACCURATE IMPLICIT METHODS FOR THE PRICING OF BARRIER OPTIONS

NDOGMO, J.C. AND NTWIGA, D.B.

**ABSTRACT.** This paper deals with a high-order accurate implicit finite-difference approach to the pricing of barrier options. In this way various types of barrier options are priced, including barrier options paying rebates, and options on dividend-paying-stocks. Moreover, the barriers may be monitored either continuously or discretely. In addition to the high-order accuracy of the scheme, and the stretching effect of the coordinate transformation, the main feature of this approach lies on a probability-based optimal determination of boundary conditions. This leads to much faster and accurate results when compared with similar pricing approaches. The strength of the present scheme is particularly demonstrated in the valuation of discretely monitored barrier options where it yields values closest to those obtained from the only semi-analytical valuation method available.

## 1. INTRODUCTION

Barrier options are a type of path-dependent options whose values depend on the specific path followed by the underlying asset during the option's life, and w.r.t. some specified asset values, usually referred to as barriers. These options are exotic derivatives traded in over-the-counter markets and they can therefore be tailored to specific customer needs. Moreover, the additional constraints imposed on them by the barrier makes them a much cheaper and attractive product than the standard options. Barriers can also be added to any existing type of standard or exotic option. The barrier option market has thus been expanding rapidly and it has been estimated [19] that it has doubled every year since 1992. In parallel with this development, a large number of newly designed barrier options have been trading very actively in financial markets [7, 30].

Analytical formulas exist for most of the standard barrier options. Rubinstein and Reiner [28], Rich [26], and Kunitomo and Ikeda [21] derived analytical formulas for a variety of standard knock-in and knock-out European options with full barriers. Heynen and Kat [18] obtained similar formulas for some special types of barrier options, namely the partial barrier options, and for so-called outside barrier options where it is another variable different from the underlying asset which determines whether the option knocks in or out. Closed-form solutions for double barrier options, some of which are time-dependent, have been obtained [21, 15, 25]. The extension of these formulas to the more complex case of American-style barrier options has been undertaken by Broadie and Detemple [6], Gao *et al.* [14], as

---

2000 *Mathematics Subject Classification.* 65M06 91B28 65C30 .

*Key words and phrases.* High-order accurate scheme; Probability-based optimal boundary; Barrier monitoring; Discretely monitored barriers.

well as Haug [16]. However, all the formulas obtained in such extensions are only closed-form approximations.

Despite all these efforts to derive analytical pricing formulas for barrier options, there is still no analytical formulas available for large classes of both European- and America-style barrier options [16, 21]. Although Merton [23] proposed the closed-form solution for the continuously monitored down-and-out barrier option in 1973, it's only in the 1990's that valuation formulas were obtained for other variants of this European-style option [28, 26, 18, 21]. This is simply because the valuation of financial options has led to mathematical models which are most often challenging to solve. For instance, for most of the complex options, there are no analytical formulas available, and almost all formulas have been obtained under the assumptions that, amongst others, the underlying asset price has a lognormal distribution with constant drift and volatility parameters, and that there are no transaction costs [28, 16]. However, as empirical evidence suggest the contrary, new models with stochastic or time-dependent volatilities, or including transaction costs have been designed and implemented. Nevertheless, these attempts to improve on the assumptions underlying the derivation of analytical formulas have been made mostly for standard American options [17, 11, 20].

For the valuation of options, and exotic options in particular, numerical methods remain a tool of choice. This is first justified by the fact that the number of exotic options that can be designed is limitless, and as new products enter the market one of the most practical way, if not the only available means to price them, are quite often the numerical methods. They are also a convenient benchmark for testing the validity of analytical formulas, especially as they become available. There are even instances where they are faster than analytical methods, even those analytical methods involving fast converging infinite sums, when the required accuracy isn't too high.

As a numerical method for option valuation, the lattice methods have been used extensively, and for barrier options it appears however that they are essentially useless without the proper positioning of the barrier which must line-up with the tree nodes. Despite all the techniques that have been developed to improve on lattice methods, they are still quite computer-intensive [16]. Monte Carlo Methods have been considered as inflexible and unreliable for option pricing, until the last decade where they yielded more promising results based on innovative techniques which are now a topic of current research. Barraquand and Martineau [2] amongst others, obtained in this context some interesting results for multi-asset American options. The most commonly used numerical method in option pricing these days appears to be the finite difference methods. They have an acceptable computational cost when an appropriate implicit method is used (see [30, 22, 20]). They can also be extended to cater for American-style options, by formulating them as linear complementary problems.

In this paper we consider an implicit finite difference approach to the valuation of barrier options. These barrier options may have various features including double barriers, dividend-paying-stocks, rebate payments, or some combination of these. Barriers may be monitored either continuously or discretely. We use a well-known  $\theta$ -method which is fourth-order accurate in space and second-order accurate in time, by relating the parameter  $\theta$  to the mesh sizes. In addition to the high-order accurate scheme and the stretching effect of the coordinate transformation used,

the strength of this approach lies on a probability-based optimal determination of the boundary conditions, along which the option values are known exactly. In this way, with a reasonable accuracy and for the most practical considerations, we are generally able to use fewer than 20 asset prices and 20 time steps per year to value most of the barrier options, especially when the barrier is continuously applied. However, the efficiency of our approach is much clearly demonstrated in the case of discretely monitored barrier options, when we compare the results we obtained with that of several other authors. As usual, due to some parity considerations, we shall focus our attention only on knock-out call options.

This paper is organized as follows. In Section 2 we discuss the mathematical model for valuing barrier options. Section 3 is devoted to the discretization of the modeling differential equation, while Section 4 discusses applications of the resulting implicit scheme to the various types of barriers options, and Section 5 reports the corresponding numerical results.

## 2. OPTION PRICING MODEL

We make the usual assumption that the underlying asset price  $S$  has a geometric Brownian motion, with drift and volatility parameters  $\mu$  and  $\sigma$ , respectively. Thus the process followed by  $S$  can be written with the usual notation and in terms of the Wiener process  $W$  as

$$dS = \mu dt + \sigma dW. \tag{2.1}$$

The price  $f = f(S, t)$  of a European option contingent on  $S$  must then satisfy the Black-Scholes differential equation

$$\mathcal{L} \cdot f = 0 \tag{2.2}$$

where the partial differential operator  $\mathcal{L}$  is given by

$$\mathcal{L} := \frac{\partial}{\partial t} + \mu S \frac{\partial}{\partial S} + \frac{1}{2} S^2 \sigma^2 \frac{\partial^2}{\partial S^2} - r, \tag{2.3}$$

and where  $r$  denotes the risk-free interest rate. We shall usually assume that the underlying asset price pays a continuous dividend yield at a continuous rate of  $q$  per year, and as we are placing ourselves in the traditional risk-neutral world in which the market price of risk is zero, we shall have in this case  $\mu = r - q$ .

Thanks to the put-call parity for European options, and also to the similar parity relation between knock-ins and knock-outs, we shall consider only knock-out call options. To begin with, let  $B$  denote the constant barrier value for a down-and-out barrier option. Since the value of the option at expiration time  $T$  is its payoff  $\text{Max}(S - K, 0)$ , where  $K$  is the strike price of the option, the initial condition for equation (2.2) is given by

$$f(S, T) = \text{Max}(S - K, 0), \quad \text{for } S > B. \tag{2.4}$$

The corresponding boundary conditions follow from the properties of call options. In the simplest case where the constant barrier value  $B$  is continuously applied, denoting by  $Rb$  the rebate received if the barrier is ever breached, the boundary conditions are

$$f(B, t) = Rb, \quad \forall t \quad (2.5)$$

$$f(S, t) \sim S, \quad \forall t, \quad \text{as } S \rightarrow \infty. \quad (2.6)$$

It should be noted that boundary condition (2.6) which is usually used for the valuation of call options is not suitable for an optimal algorithm, in particular because the value of  $S$  in that condition is generally exceedingly large, and the resulting equality is only an approximation, and all these tend to slow down the valuation algorithm. We shall therefore always strive in this paper to find optimal boundaries of the solution domain along which the option values are known exactly, and which also yield an optimal truncation of the solution domain.

The Black-Scholes equation (2.2) can be analyzed directly for the valuation of barrier options, as for example in [4] and [30]. However, there is a numerically more effective coordinate transformation that we shall adopt here, and which is obtained by first setting

$$x = \ln(S/K), \quad (2.7)$$

$$\tau = \frac{\sigma^2}{2}(T - t). \quad (2.8)$$

Since for all practical considerations the underlying price range generally lies in a subinterval of  $(K/3, 3K)$ , it appears that (2.7) restricts the underlying asset price in the  $x$ -coordinate to range most often in a small interval such as  $(-1.099, 1.099)$ . On the other hand, (2.8) not only transforms (2.2) into a forward-time problem, but it also has the advantage of shrinking the time range. Under the change of coordinates (2.7) and (2.8), equation (2.2) is transformed into

$$\frac{\partial f}{\partial \tau} = \frac{\partial^2 f}{\partial x^2} + (\nu - 1) \frac{\partial f}{\partial x} - \nu_1 f$$

where  $\nu = 2\mu/\sigma^2$ , and  $\nu_1 = 2r/\sigma^2$ . So,  $\nu = \nu_1 - \nu_2$ , where  $\nu_2 = 2q/\sigma^2$ . Here  $\nu_1$  and  $\nu_2$  are the only two non-dimensional parameters of the Black-Scholes equation for dividend-paying-assets. To discard the terms in  $f$  and  $\partial f/\partial x$  in this last differential equation, we now make a change of the dependent variable by setting

$$f(S, t) = Ke^{\alpha x + \gamma \tau} u(x, \tau), \quad (2.9)$$

where  $\alpha = -\frac{1}{2}(\nu - 1)$  and  $\gamma = -\frac{1}{4}(\nu + 1)^2 - \nu_2$ . This last change of variables reduces the original equation (2.2) to the diffusion equation

$$\frac{\partial u}{\partial \tau} = \frac{\partial^2 u}{\partial x^2}. \quad (2.10)$$

Letting  $x_b = \ln(B/K)$ , the initial and boundary conditions given earlier are also transformed into the following expressions in the  $(x, \tau)$ -coordinates.

$$u(x, 0) = \text{Max} \left( e^{(1/2)(\nu+1)x} - e^{(1/2)(\nu-1)x}, 0 \right), \quad x > x_b \quad (2.11a)$$

$$u(x, \tau) \sim e^{(1-\alpha)x - \gamma\tau}, \quad \text{as } x \rightarrow \infty \quad (2.11b)$$

and

$$u(x_b, \tau) = \frac{Rb}{K} e^{-(\alpha x_b + \gamma\tau)}. \quad (2.11c)$$

It is worth noting at this point that the change of variable (2.9) is also very convenient for an efficient numerical algorithm. Indeed, it gives the final solution as a scalar multiple of the numerically computed factor  $u(x, \tau)$ , where the scalar  $Ke^{\alpha x + \gamma \tau}$  is known exactly and so, does not involve any error. In this way any error expansion due to transformation (2.9) will tend to be minimized.

### 3. FINITE DIFFERENCE SCHEME

Denote by  $h = \Delta x$  and  $k = \Delta \tau$  the mesh sizes in the space and the time directions, respectively. Denote also by  $U_j^n$  the discrete approximation of  $u(x, \tau)$  at the grid node  $(x_j, t_n)$ , where  $x_j = j\Delta x$ , and  $t_n = n\Delta t$ . Let  $\delta_x^2$  be the difference operator given by  $\delta_x^2 U_j^n = U_{j-1}^n - 2U_j^n + U_{j+1}^n$ . For the discretization of the reduced equation (2.10) we choose the two-time level, three-space-point scheme

$$\frac{U_j^{n+1} - U_j^n}{\Delta t} = \frac{1}{(\Delta x)^2} (\theta \delta_x^2 U_j^{n+1} + (1 - \theta) \delta_x^2 U_j^n) \quad (3.1)$$

also called weighted average approximation or  $\theta$ -method. The weight  $\theta$  in this expression is assumed to satisfy the condition  $0 \leq \theta \leq 1$ , in order to avoid negative weights. The values  $\theta = 0$  and  $\theta = 1$  give the explicit scheme and the fully implicit scheme, respectively. If we let  $\beta = \Delta t / (\Delta x)^2$ , i.e.  $\beta = k/h^2$ , then for  $0 \leq \theta < \frac{1}{2}$ , the scheme (3.1) is stable if and only if  $\beta \leq 1/2(1 - 2\theta)$ . For  $\frac{1}{2} \leq \theta \leq 1$ , it is stable for all values of  $\beta$ . For this scheme, the truncation error, i.e. the amount by which the exact solution of the differential equation does not satisfy the discrete approximation (3.1), is generally of first order accuracy in  $\Delta t$ , while the popular Crank-Nicolson scheme which corresponds to  $\theta = 1/2$  is second-order accurate in both  $\Delta t$  and  $\Delta x$ .

For a much higher accuracy of the finite difference scheme (FDS) (3.1), we shall relate in this paper the choice of the parameter  $\theta$  to the values of  $\Delta x$  and  $\Delta t$  of the grid line spacings. More precisely, we shall assume that

$$\theta = \frac{1}{2} - \frac{1}{12\beta}. \quad (3.2)$$

It is well-known that the resulting scheme is  $O((\Delta t)^2 + (\Delta x)^4)$ , i.e. second-order accurate in time and fourth order accurate in space (see e.g. [24]). Such a scheme has been used in [22] for the valuation of American options with error correction at the critical boundary, leading to results that are comparatively more accurate than the standard ones found in the literature. However, this specific weighted average scheme has not yet been applied to the valuation of barrier options, to the best of our knowledge. Zvan *et al* used a method called point-distributed finite volume scheme in [30] to directly discretize the Black-Scholes equation, but that method is only first order accurate in time, and the paper does not comment on the speed (in terms of number of time steps) of the scheme for achieving a given level of accuracy.

Since  $\beta$  is positive, condition (3.2) restricts  $\theta$  to the interval  $[0, 1/2)$ , but the condition for stability  $\beta \leq 1/2(1 - 2\theta)$  is always satisfied in this case. Moreover, the condition  $0 \leq \theta$  implies that

$$(\Delta x)^2 \leq 6\Delta t. \quad (3.3)$$

This in practical terms means that even by requesting (3.2) to hold, we can still take large time steps while maintaining accuracy and stability.

If we denote by  $M$  and  $L$  the number of space- and time-intervals, respectively, in the solution grid, and by  $W_{h,k}$  the finite difference operator given by

$$W_{h,k} \cdot U_j^n = -\beta\theta U_{j-1}^n + (1 + 2\beta\theta)U_j^n - \beta\theta U_{j+1}^n,$$

then an expansion of the discretized equation (3.1) leads to a linear algebraic system of equations of the form

$$W_{h,k} \cdot U_j^{n+1} = W_{h,k} \cdot U_j^n, \quad \text{for } n = 0, \dots, L-1 \text{ and } j = 1, \dots, M-1. \quad (3.4)$$

The system (3.4) can be written in terms of tridiagonal matrices and we shall solve it with the Thomas algorithm which includes Gaussian elimination without pivoting.

#### 4. NUMERICAL SOLUTION FOR BARRIER OPTIONS

We discuss in this section the application of the FDS described above to the derivation of a numerical solution to the pricing problem for barrier options.

**4.1. Overview.** As already indicated, we shall always implement whenever possible in this paper an optimal truncation of the solution domain by replacing the approximate boundary condition of the form (2.6), or (2.11b) equivalently, with a boundary condition for which both the option value is known exactly and the resulting solution domain is the smallest possible. Let  $S_0$  be the initial price of the underlying and  $S = S_t$  the price of the underlying at a time  $t$ ,  $0 < t \leq T$ . In the case of a down-and-out call option, the probability  $P(S_t > B)$  that the barrier will not be breached at time  $t$  is given by

$$P(S_t > B) = \Phi(a^*), \quad (4.1)$$

where  $\Phi$  is the standard normal distribution function and

$$a^* = (\ln(S_0/B) + \mu^*t)/\sigma\sqrt{t}, \quad \text{with } \mu^* = \mu - \sigma^2/2.$$

Let  $\delta$  be the smallest number such that  $\Phi(\delta)$  has numerical value 1. The value of  $\delta$  depends on the level of accuracy required and also on the computing system used for the calculations. An appropriate value for  $\delta$  usually lies in the interval (3.7, 6.5), depending on the level of accuracy required. For a given parameter set, the minimum value of  $S_0$  which guarantees that the barrier will not be breached at time  $t$  is given by the inequality  $a^* \geq \delta$ , or equivalently by  $S_0 \geq Be^{\delta\sigma\sqrt{t} - \mu^*t}$ . Now, let  $t_p$  be the turning point of the function  $t \mapsto \delta\sigma\sqrt{t} - \mu^*t$ , and denote by  $S_m$  the minimum value of the current stock price  $S_0$  above which the barrier becomes worthless, and set  $x_m = \ln(S_m/K)$ . Then it is easy to see that

$$x_m = \begin{cases} x_b + \delta\sigma\sqrt{T} - \mu^*T, & \text{if } \mu^* \leq 0 \text{ or } t_p \geq T \\ x_b + \delta\sigma\sqrt{t_p} - \mu^*t_p, & \text{otherwise.} \end{cases} \quad (4.2)$$

For any value of  $S_0$  above  $S_m$ , or equivalently for any value of  $x_0$  above  $x_m$ , where  $x_0 = \ln(S_0/K)$ , the barrier is worthless and the option behaves exactly as a standard option. In particular, the corresponding option value along the boundary  $S = S_m$  or above this boundary is given by the well-known Black-Scholes formula for European call options.

It therefore follows from Equations (2.5), (2.8) and (4.2) that the solution domain for  $u(x, \tau)$  reduces to the rectangle  $[x_b, x_m] \times [0, \frac{\sigma^2}{2}T]$ . Similarly for an up-and-out

barrier option, if we let  $S_m$  denote the maximum value of the current underlying asset price below which the barrier becomes worthless, then  $x_m = \ln(S_m/K)$  is given by

$$x_m = \begin{cases} x_b - \delta\sigma\sqrt{T} - \mu^*T, & \text{if } \mu^* \geq 0 \text{ or } t_p \geq T \\ x_b - \delta\sigma\sqrt{t_p} - \mu^*t_p, & \text{otherwise.} \end{cases} \quad (4.3)$$

In this case the optimal solution domain reduces to the rectangle  $[x_m, x_b] \times [0, \frac{\sigma^2}{2}T]$ . This optimal determination of the boundary conditions has several applications, including the classification of double barrier options. A similar determination of optimal boundary conditions can be achieved for time-varying barriers, as opposed to the constant barriers we have discussed here. Note that by construction we have  $x_m > x_b$  in (4.2) and  $x_m < x_b$  in (4.3)

Our determination of the numerical solution for a pricing problem will amount to calculating  $u(x_0, \tau_M)$ , where  $\tau_M = \frac{\sigma^2}{2}T$ , and this may require interpolation if  $x_0$  does not line up with a grid line. However, for  $M$  large, it is always possible to slightly enlarge the range of the spacial variable  $x$  without affecting the performance of the algorithm in any way, just by adjusting the value of  $x_m$  by a fraction of the grid increment. By so doing, we can always line up  $x_0$  with a grid point, and such adjustment of  $x_m$  is feasible when for instance the grid increment  $h = \Delta x$  is small. We shall therefore combine these two techniques in our calculation of  $u(x_0, \tau_M)$ .

The price of barrier options often displays some singularities near the barrier value and it is therefore customary in a finite difference pricing approach for these options to use adaptive grids in an attempt to achieve the required accuracy of the numerical solution with a smaller number of mesh points, i.e. with a faster algorithm. Suppose that the grid increment  $h = \Delta x$  of the spacial variable  $x$  is non constant and denote by  $h_j = x_{j+1} - x_j$  the  $j$ th grid increment, where the  $x'_j$ s are grid points in the  $x$ -direction. The number  $q_j = h_j/h_{j-1}$  is often called non uniformity parameter of the difference grid [1]. A direct substitution of the non constant increment  $h_j$  into the FDS (3.1) gives rise to the nonuniform version of equation (3.4). A similar but much simpler discretization of equation (2.10) can be derived for a nonuniform time stepping. For the nonuniform discretization of either of the variables, we used a geometric progression. Thus for the space variable, we set  $h_1 = h$ ,  $h_j = R^{j-1}h$  for some positive numbers  $R$  and  $h$ . Here,  $R$  turns out to be the non uniformity parameter and the  $h_j$ 's form a geometric progression with common ratio  $R$ . Values of  $R$  not close to 1 will lead to instability of the numerical solution, while for  $R$  close to 1 the resulting scheme will tend to be stable [1].

A two-dimensional grid made up of  $M$  space intervals and  $L$  time intervals will be referred to as a grid of mesh (size)  $M \times L$ . In the case of the *fds* that we are considering,  $L$  and  $M$  are to be so chosen that (3.3) is satisfied, and this is easily achieved by letting  $L = M$ . In some very rare cases (e.g when  $\sigma \geq 35\%$ ), the occurrence of negative option prices at the intermediary time steps might become persistent and slow down the convergence of the scheme. This type of difficulty is also easily resolved by letting  $L$  be slightly larger than  $M$ , say  $L = 1.5M$ .

It should be noted that our algorithm for the implementation of the optimal boundary condition shares some similarities with the method for finding the conditional expectation estimator in the Monte Carlo simulation of a down-and-in barrier option [27]. Indeed, in such a Monte Carlo valuation, as soon as the barrier is breached, the simulation run is ended, and the corresponding estimator is the

Black-Scholes value for the resulting option parameters. In the same way for the finite difference scheme, as soon as we are certain that the initial price is sufficiently far away for the barrier to become worthless, the corresponding option value is its Black-Scholes value.

**4.2. Discretely monitored barriers.** In the case of discretely sampled barriers, we assume that barrier monitoring occurs either on a daily basis or on a weekly basis. We adopt a day count convention which will allow a comparison of our numerical results with others at our disposal by letting a year consist of 50 weeks, and a week to consist of 5 days, so a year has 250 days. For the numerical solution, we let  $\rho$  be the number of time steps implemented between two consecutive monitoring dates, so that the total number of time steps is given by  $L = N\rho$ , where  $N$  is the number of monitoring dates during the option's life. As is well-known [4, 8], for increased accuracy and improved convergence, we shall place the barrier itself midway between grid points.

## 5. NUMERICAL RESULTS

We start by showing the result of the performance test for the proposed optimal truncation of the solution domain. In most papers where approximate conditions of the form (2.6) are used to determine boundary conditions in barrier option pricing problems, the value used for  $S_{\max}$ , the maximum asset price in the solution domain, is usually not indicated. That is the case for instance in [30] and [4]. However, by rewriting and implementing the same algorithm described in the latter paper under the scheme termed modified explicit finite difference (MEFD) in that paper, we've found by trial and error that choosing  $S_{\max} = 2S_0 + 200$  gives exactly the same results as those in Table 1 and Table 4 of the said paper. This value of  $S_{\max}$  also turns out to give the best results for the parameter sets considered in that same paper. Other choices for  $S_{\max}$  which are commonly used for a similar range of data are  $S_{\max} = 2S_0$ , or  $S_{\max} = S_0 + 100$ , as in [9] and [22]. However, inappropriate choices for  $S_{\max}$  lead to very poor results as we show in Table 1.

Contrary to conditions of the form given by equations (4.2)-(4.3) that yield a systematic determination of the optimal boundary conditions, there is certainly no formula available for the best choice of  $S_{\max}$  and it's value is usually determined only by trial and error. For two different values of  $S_0$ , Table 1 compares for a down-and-out barrier option the convergence rates under the MEFD scheme and under our optimal boundary explicit scheme (OBES) using data from Table 1 of [4]. The two different formulas used for  $S_{\max}$  are  $S_{\max} = 2S_0 + 200$  and  $S_{\max} = 2S_0$ . The parameter set is  $T = 1$ ,  $K = 100$ ,  $B = 90$ ,  $\sigma = 0.25$ , and  $r = 0.10$ . For the explicit scheme used, the mesh size is determined by a single parameter  $L$  representing the number of required time steps, because of the usual stability conditions relating the time and the space increments in an explicit scheme. Moreover, this constraint for the MEFD scheme upon which all explicit schemes considered in this paper are based is given by

$$\Delta y = \lambda \sigma \sqrt{\Delta t}, \quad (5.1)$$

where  $y = \log(S)$ . Numbers within parentheses in Table 1 are CPU times. All runs in this paper were carried out on a conventional Pentium Celeron 2.40 Ghz CPU. In all the tables the parameters  $q$  and  $Rb$  are assumed to be zero, unless otherwise indicated.



TABLE 1. Comparison of the accuracy and the CPU time under the optimal boundary explicit scheme (OBES) and the MEFD of [4] for a down-and-out call. The fixed parameter set is  $T = 1, K = 100, B = 90, \sigma = 0.25, r = 0.10$ . Numbers within parentheses are CPU times.

Mesh (L)	$S_0 = 95$		$S_0 = 91$		
	Closed-Form: 5.9968		Closed-Form: 1.2738		
	OBES	MEFD	OBES	MEFD	
		$S_{\max} = 2S_0 + 200$	$S_{\max} = 2S_0$		$S_{\max} = 2S_0 + 200$
50	6.01109 (0.36)	6.0111 (0.344)	6.8299	1.2654 (0.39)	1.2654 (0.33)
100	5.9984 (0.53)	5.9984 (0.44)	6.8603	1.2704 (0.53)	1.2704 (0.47)
150	5.9965 (2.09)	5.9997 (2.33)	6.7449	1.2719 (2.203)	1.2719 (2.42)
200	5.9993 (2.54)	5.9993 (2.70)	6.6897	1.2725 (2.58)	1.2726 (2.85)
700	5.9970 (15.81)	5.9970 (17.766)	6.74	1.2738 (15.75)	1.2738 (18.16)
800	5.9972 (19.20)	5.9972 (21.906)	6.78	1.2739 (19.44)	1.2739 (22.30)
900	5.9973 (10.703)	5.9973 (12.047)	6.80	1.2739 (10.922)	1.2739 (11.625)
1000	5.9969 (33.86)	5.9969 (40.59)	6.7991	1.2739 (34.31)	1.2739 (42.25)
2000	5.9970 (72.67)	5.9970 (85.97)	6.7949	1.2738 (75.12)	1.2738 (85.797)
3000	5.9969 (189.34)	5.9969 (238.141)	6.7718	1.2738 (192.062)	1.2738 (236.66)
4000	5.9969 (263.28)	5.9969 (320.187)	6.8020	1.2738 (268.39)	1.2739 (335.31)

Columns 2 and 3 of Table 1 show that the OBES and the MEFD schemes give essentially the same option values for the given parameter set, when  $S_{\max} = 2S_0 + 200$  in the MEFD. However, our OBES appears to be up to 20% faster for all significant number of time steps (i.e. for  $L \geq 150$ ). For small values of  $L$  below 150, the excess amount of time used in the OBES to calculate the option values at different time steps on the upper boundary determined by  $S_m$  exceeds the excess time required in the MEFD to implement the additional time steps. But this is of no importance as regards the performance of the schemes, as for explicit schemes accuracy is generally not achieved below  $L = 1000$  steps. The same conclusion applies when comparing columns 5 and 6 of the table.

A comparison of Column 3 and 4 of the same table shows the importance of choosing an appropriate value for  $S_{\max}$ . Indeed, the same calculations in Column 3 when done in Column 4 with  $S_{\max} = 2S_0$ , which as already mentioned is a commonly used value for similar parameter sets in option pricing problems, reveals that the scheme certainly does not even converge to the closed-form value of 5.9968. However, even for those values of  $S_{\max}$  for which the MEFD does converge, there is no systematic way for finding them.

TABLE 2. Effect of volatility on the performance of the OBES and the MEFD of [4] for a down-and-out call with fixed parameters  $S_0 = 95, T = 1, K = 100, B = 90$ , and  $r = 0.10$ .

	Mesh	OBES	MEFD		Closed-form
			$S_{\max} = 2S_0 + 200$	$S_{\max} = 2S_0$	
$\sigma = 0.25$	$200 \times 200$	5.9993	5.9993	6.6897	5.9968
	$2000 \times 2000$	5.9970	5.9970	6.7949	
$\sigma = 0.30$	$200 \times 200$	5.9071	5.9075	7.6180	5.9060
	$2000 \times 2000$	5.9061	5.9065	7.7124	
$\sigma = 0.40$	$200 \times 200$	5.7498	5.7802	9.2320	5.7502
	$2000 \times 2000$	5.7503	5.7789	9.5294	

The validity of our optimal determination of boundary conditions is further demonstrated by the effect of volatility in Table 2. Indeed, this experiment shows that as the volatility increases, the MEFD becomes more and more inaccurate for almost every possible choice of  $S_{\max}$ , and does not even tend to converge for values of  $\sigma$  above 40%. On the other hand the OBES is perfectly unaffected by any change in the value of  $\sigma$ . Indeed, for large values of  $\sigma$ , the approximation  $f(S, t) \sim S$  for all  $t$  is only tolerated in the MEFD for much larger values of  $S$ . We've found that by adequately increasing the value of  $S_{\max}$  for a larger value of  $\sigma$ , convergence under the MEFD can still be achieved, but at the expense of much longer computing times and additional trial and error experiments to find  $S_{\max}$ . Some complications might also arise in the choice of  $S_{\max}$ , due to the constraint (5.1). As for the OBES, any change in the value of  $\sigma$  is fully captured by both  $S_m$  and the corresponding Black-Scholes value, so that the OBES remains totally unaffected by such changes.

The efficacy of combining the high-order accurate implicit scheme determined by equation (3.2), with the stretching coordinates transformation given by (2.7)-(2.8), and the optimal truncation of the solution domain is first tested for a down-and-out barrier call option in Table 3. We denote by HOBIS (high-order optimal boundary implicit scheme) the high-order implicit finite difference scheme that applies the

TABLE 3. Down-and-out option values for initial asset prices closest to the upper boundary (U), the lower boundary (L) or at midway (M). The fixed parameters are  $K = 150$ , and  $B = 180$ . Numbers within parentheses are CPU times.

		$T = 0.25, \sigma = 0.20,$ $r = 0.05$				$T = 1, \sigma = 0.45,$ $r = 0.07$		
		$S_m = 271.906$ $x_m - x_b = 0.4125$				$S_m = 1345.08$ $x_m - x_b = 2.0112$		
		$S_0$	Closed- Form	HOBIS Mesh	HABIS Mesh	$S_0$	Closed- Form	HOBIS Mesh
U		271.905	123.768	$3 \times 1$ (0.00)	$25 \times 25$ (0.05)	1345.07	1205.21	$2 \times 1$
		271.902	123.765	$3 \times 1$	$25 \times 25$	1345.00	1205.14	$3 \times 1$
		270.000	121.862	$10 \times 10$	$25 \times 25$	1344.00	1204.14	$7 \times 7$
		265.000	116.861	$12 \times 12$	$25 \times 25$	1340.00	1200.14	$10 \times 10$
L		180.001	0.0026	$6 \times 6$ (0.03)	$30 \times 30$	180.001	0.0015	$3 \times 1$
		180.010	0.0264	$11 \times 11$	$30 \times 30$	180.01	0.0015	$3 \times 1$
		181.000	2.6297	$135 \times 135$ (1.20)	$400 \times 400$ (14.25)	181.00	1.4817	$95 \times 95$ (0.55)
M		225.953	77.2335	$95 \times 95$ (0.53)	$600 \times 600$ (39.26)	762.54	622.632	$85 \times 85$ (0.52)

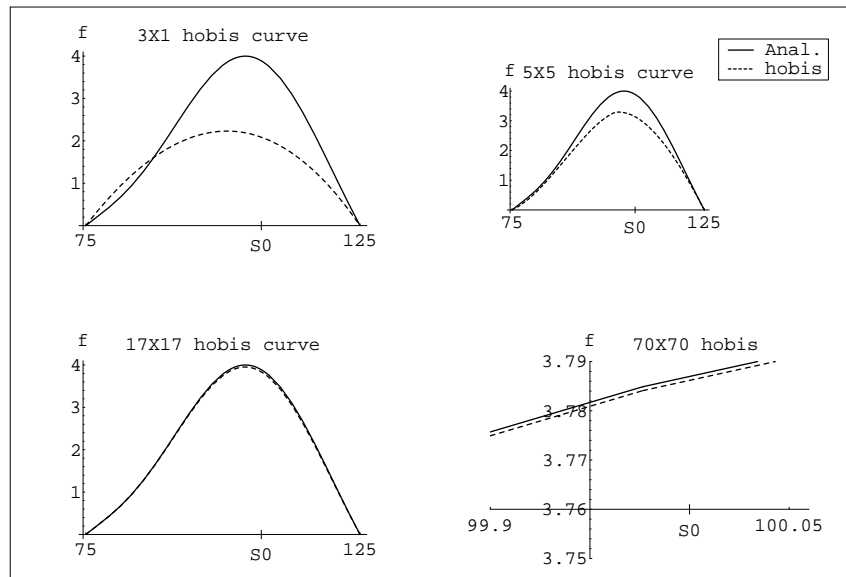
optimal determination of the boundary conditions, while the corresponding scheme in which a boundary condition is determined by the approximate condition (2.6) will be referred to as HABIS (high-order approximate boundary implicit scheme).

A striking feature of the high-order accurate HOBIS is its fastest convergence for initial asset prices closest to boundaries of the solution domain. For initial asset values closest to  $S_m$  on the upper boundary (U), the minimum mesh size that returns the analytical option price is  $2 \times 1$  and corresponds to a CPU time of 0.00 seconds. For values closest to the barrier on the lower boundary (L), the minimum mesh size is  $7 \times 7$  and corresponds to a CPU time of 0.02 seconds. This performance is clearly due to the exactness of option values at the boundaries in combination with the fact that interpolation yields best results for points closest to known function values. But this is also a consequence of the coordinates transformation (in the first set of data with  $\sigma = 0.20$  in Table 3,  $x_m - x_b = 0.4125 < 1$ ), the higher-order accuracy of the scheme that forces all error less than one to quickly disappear, and the implicit nature of the scheme that also tends to quickly reduce any error. For instance, in the second set of data in Table 3 with  $\sigma = 0.45$ , and  $S_0 = 1345.00$ , although the space increment is

$$\Delta x = 2.011/2 = 1.005 > 1,$$

all significant errors have disappeared by the completion of the first time step. The table also shows as expected that the more we move away from the boundaries, the higher the error tends to become in option values with a fixed mesh size. We have therefore also indicated the minimum CPU time required for initial values midway (M) between the boundaries, and we can reasonably argue that for any given scheme and any parameter set, the maximum CPU time for all values of  $S_0$  in the solution domain is close to the maximum CPU time obtained for  $S_0$  close to the boundaries and at midway. This means for instance that for the first set of data with  $\sigma = 0.20$ , and the second set of data with  $\sigma = 0.45$ , to within four significant digits of accuracy, the maximum CPU time is close to 1.20s and 0.55s, respectively. It should be noted that this is also the maximum CPU time for any possible value of the initial price. Indeed, another feature of the optimal boundary condition is to determine exactly when a barrier becomes worthless for a given value of  $S_0$ , so its value is reduced to the corresponding vanilla Black-Scholes value. More precisely, by construction of  $S_m$ , whenever  $S_0 \geq S_m$  the barrier option value is the vanilla Black-Scholes value, and so any scheme (explicit, implicit or otherwise) based on the optimal boundary returns the option value in zero seconds for such values of  $S_0$ .

FIGURE 1. Convergence patterns under the HO-BIS for a double knock-out. The parameter set is  $S_0 = 100, T = 0.5, K = 100, B_l = 75, B_u = 125, \sigma = 0.20$  and  $r = 0.10$ . All absolute errors are less than 10% with a  $17 \times 17$  mesh, and less than  $2 \times 10^{-3}$  with a  $70 \times 70$  mesh.



The 5th column of Table 3 shows that implementing the same high-order accurate implicit scheme by using the approximate boundary condition of the form (2.6) leads to much more inaccurate results and requires about 10 times more computing time, although the value of  $S_{\max} = 2S_0 + 200$  appears to be the best choice for all sets of

parameters considered. This numerical experimentation confirms the fact that the superior accuracy of the HOBIS is valid for all finite difference schemes.

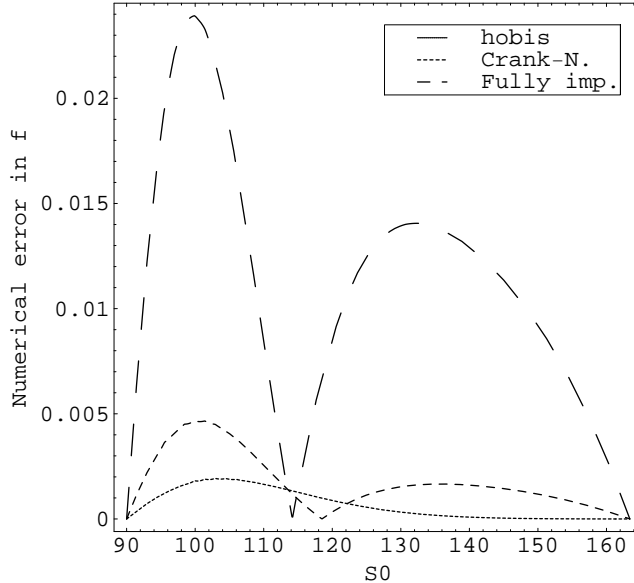
The HOBIS curves depicted in Figure 1 for a double knock-out also display a similar trend of convergence described in Table 3, in which accuracy is much quickly achieved for points closer to the boundaries of the solution domain, while the middle point returns the most coarse value (at least for the first few mesh sizes). The parameter set for this figure is  $S_0 = 100, T = 0.5, K = 100, B_l = 75, B_u = 125, \sigma = 0.20$  and  $r = 0.10$ . The figure clearly shows the global accuracy of the HOBIS for different mesh sizes. For a  $17 \times 17$  mesh size, the HOBIS curve is essentially indistinguishable from the analytical curve and the maximum absolute error is  $5.1 \times 10^{-2}$ . This error reduces to  $3.0 \times 10^{-3}$  for a  $70 \times 70$  mesh size.

TABLE 4. Maximum absolute error under the HOBIS for continuously monitored down-and-out and double knock-out calls. The fixed parameter sets are  $K = 100, B = 90, r = 0.10$  for the down-and-out call and  $K = 100, B_l = 75, B_u = 125, r = 0.10$  for the double knock-out call. The maximum absolute error is that on the  $M + 1$  computed option prices for any given mesh size of the form  $M \times L$ .

$\sigma$	DOWN-AND-OUT CALL			DOUBLE KNOCK-OUT CALL		
	para- meters	mesh	error	para- meters	mesh	error
0.15	$T = 0.5$	$7 \times 7$	$2.4 \times 10^{-2}$	$T = 0.5$	$20 \times 20$	$7.9 \times 10^{-2}$
	$T = 0.5$	$20 \times 20$	$1.3 \times 10^{-3}$	$T = 0.5$	$100 \times 100$	$3.1 \times 10^{-3}$
	$T = 0.5$	$100 \times 100$	$3.0 \times 10^{-5}$	$T = 0.5$	$200 \times 200$	$7.8 \times 10^{-4}$
	$T = 1$	$100 \times 100$	$3.6 \times 10^{-5}$	$T = 1$	$200 \times 200$	$4.0 \times 10^{-4}$
	$\{T = 1, Rb = 3\}$	$100 \times 100$	$5.6 \times 10^{-5}$	$T = 0.1$	$200 \times 200$	$3.5 \times 10^{-3}$
0.35	$T = 1$	$100 \times 100$	$2.6 \times 10^{-4}$	$T = 1$	$200 \times 200$	$6.3 \times 10^{-2}$

For almost all typical model parameters, the HOBIS and analytical curves are essentially indistinguishable in the case of a down-and-out call, even for the smallest  $3 \times 1$  mesh size. We've therefore given in Table 4 the maximum absolute error on computed option prices for some given mesh sizes, and for both a down-and-out call and a double knock-out call. The table shows that the absolute HOBIS error is strictly less than  $10^{-2}$  for a  $20 \times 20$  mesh when the option is a down-and-out, and that global accuracy is much quickly achieved with a down-and-out than with a double knock-out. On the other hand there does not seem to be a simple correlation between accuracy and expiry date for a fixed mesh size in the case of the double knock-out call, at least for the three different expiry dates considered. However, it clearly transpire from the table that the HOBIS is very sensitive to volatility, especially in the case of a double knock-out call where the maximum absolute error is about 100 times larger when the volatility goes from 0.15 to 0.35. The table also shows that accuracy is a bit more expensive when the computation of option values incorporates a rebate payment.

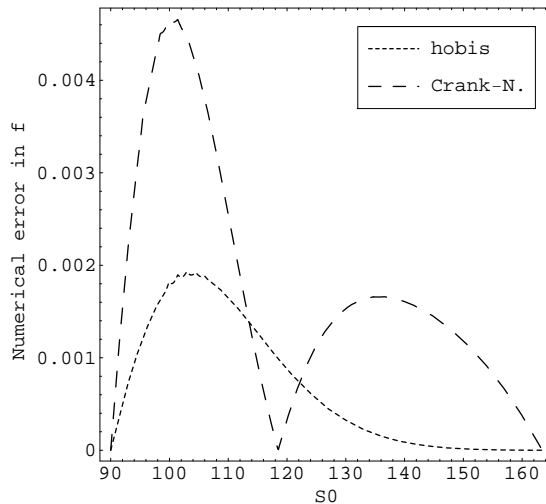
FIGURE 2. Error in the computed option prices  $f$  under the HOBIS, the Crank-Nicolson, and the fully implicit schemes. The parameter set is  $T = 0.5$ ,  $K = 100$ ,  $B = 90$ ,  $\sigma = 0.20$  and  $r = 0.10$ . The mesh size is  $40 \times 40$ .



Although the HOBIS is fourth-order accurate in the space variable and second-order accurate in the time variable while the popular Crank-Nicolson scheme is second order accurate in both the space and the time variables, this does not necessarily precludes the actual numerical implementation of these schemes to prove otherwise. We've therefore plotted against the initial price  $S_0$  in Figure 2 the numerical errors in the computed down-and-out option prices under the HOBIS, the Crank-Nicolson, and the Fully implicit schemes. The latter scheme which was used for option pricing in [30] is only first-order accurate in time. The figure shows that the HOBIS is much more accurate than the Crank-Nicolson scheme for the corresponding mesh used, and the fully implicit scheme performs very poorly compared to the HOBIS. In fact the maximum absolute errors resulting from these plots are 0.00193 for the HOBIS, 0.00466 for the Crank-Nicolson, and 0.02392 for the fully implicit scheme. The error functions for the last two schemes have each a singularity where the error tends to jump to zero, but this has essentially no effect on their performance. We have however, plotted the same error functions in Figure 3 for the two best performing schemes, namely the HOBIS and the Crank-Nicolson scheme, to clarify the difference between their levels of accuracy. Although the only mesh size used for these two figures is  $40 \times 40$ , our experimentations shows that this trend persists for all mesh sizes larger than say,  $20 \times 20$ . The common parameter set for the two figures is  $T = 0.5$ ,  $K = 100$ ,  $B = 90$ ,  $\sigma = 0.20$  and  $r = 0.10$ .

Table 5 compares HOBIS values with those reported in Table 1 and Table 2 of [30] for a down-and-out and a double knock-out call, and corresponding to values

FIGURE 3. Error in the computed option prices  $f$  under the HOBIS, and the Crank-Nicolson schemes. The parameter set is  $T = 0.5, K = 100, B = 90, \sigma = 0.20$  and  $r = 0.10$ . The mesh size is  $40 \times 40$ .



obtained in [30] using a fully implicit method of first order of accuracy (ZVAN), and in [8] using a trinomial tree method (C-V). The options parameters used are  $S = 100, T = 0.5, K = 100, \sigma = 0.20, r = 0.10$ . For the down-and-out,  $B = 99.9$ , while for the double knock-out, the lower barrier is set at  $B_l = 95$  and the upper barrier is set at  $B_u = 125$ . For continuously monitored barriers, the HOBIS values correspond to the analytical values to within the required accuracy, as are those computed by Cheuk and Vorst, while surprisingly the ZVAN values of [30] do not coincide with analytical values. Closed-form solutions for continuously monitored barrier options have been derived by various authors [23, 28, 21, 15, 25]. The HOBIS appears not only to be more accurate, but also about twice faster than the implicit scheme of [30]. In the case of discrete monitoring, the HOBIS values are essentially the same as the C-V values to within the required accuracy, but differ significantly again from those obtained using the fully implicit method of [30]. In general accuracy is very costly in terms of CPU time for discretely monitored barrier options and the computing time in Table 5 for discrete monitoring corresponding to the ZVAN column looks too little. For similar amounts of time the HOBIS returns similar option values, but does not converge to those values, and it generally requires up to a hundred of seconds to converge significantly.

Although Table 5 clearly demonstrates the higher performance of the HOBIS in terms of convergence and accuracy for continuously monitored options, it is hard to make the same conclusion from this table about discretely applied barriers, and this is largely due to the non availability of exact solutions in such cases.

We have therefore compared in Table 6 the HOBIS values for a discretely monitored down-and-out option with those taken from Table 2 of [12]. Fusai *et al* [12] have reduced the valuation problem for discretely monitored down-and-out barrier

TABLE 5. Down-and-out and double knock-out call values with continuous and discretely applied constant barriers.

Monitoring frequency	Down-and-out Call			Double Knock-out Call		
	HOBIS	ZVAN	C-V	HOBIS	ZVAN	C-V
Continuous	0.165 (0.03)	0.164 (0.05)	0.165	2.033 (0.240)	2.037 (0.48)	2.033
Daily	1.511	1.506 (13.96)	1.512	2.482	2.485 (37.93)	2.482
Weekly	3.008	2.997 (2.80)	2.963	3.006	3.012 (9.47)	2.989

The fixed options parameters are  $S = 100$ ,  $T = 0.5$ ,  $K = 100$ ,  $\sigma = 0.20$ ,  $r = 0.10$ . For the down-and-out,  $B = 99.9$ , while for the double knock-out,  $B_l = 95$ ,  $B_u = 125$ . C-v denotes results obtained in [8] while Zvan denotes results obtained in [30]. Numbers within parentheses are CPU times

options to a Wiener-Hopf integral equation, and given a formal inverse  $z$ -transform solution to this equation in terms of a special function plus infinite sums of simple functions. This however does not give rise to exact option values, as the solutions need to be evaluated numerically. In addition to the Wiener-Hopf (WH) method of [12] the other numerical methods which are compared with the HOBIS method in Table 6 are the Markov Chain method (MCH) of [10], the trinomial tree (TT) of [5], the Simpson recursive quadrature method (SQ) of [13], and the Monte Carlo simulation method (MC) of [3] with antithetic variables and  $10^8$  simulation runs. Table 6 shows that the HOBIS values are much closer to the WH values of [12] which is the only numerical method derived from an analytical solution. The table also shows that apart from the TT values in column 6, there is in general a good level of agreement between all the numerical methods. It should be noted that values from the TT method that seems to perform relatively poorly in the table are exactly the same values reported for the same discretely monitored barrier option in [8], some of which values appear in Table 5 above. This shows that for discrete monitoring, the discrepancies between the HOBIS values and other values listed in Table 5 cannot be perceived as a lack of performance of the HOBIS. In fact Table 6 simply confirms a wide spread perception that tree methods are less efficient compared to the most common numerical methods for option pricing. The fixed option parameters in Table 6 are  $S = 100$ ,  $T = 0.5$ ,  $K = 100$ ,  $\sigma = 0.20$ ,  $r = 0.10$ , and  $N$  and  $B$  denote as usual the number of monitoring dates and the barrier value, respectively.

Analytical pricing formulas for double barrier options with rebate payment has recently been obtained in [25] based on the inversion of the Laplace transform of the probability density functions by contour integration. Sidenius obtained a similar solution in [29] using an approach based on path counting. These two results are certainly among the first ones incorporating a rebate payment for continuous barrier



TABLE 6. Comparison of the HOBIS results for a discretely monitored down-and-out call. The parameter set is  $S = 100$ ,  $T = 0.5$ ,  $K = 100$ ,  $\sigma = 0.20$ ,  $r = 0.10$ , and  $N$  and  $B$  denote as usual the number of monitoring dates and the barrier value, respectively.

$N$	$B$	HOBIS	WH-IR	MCH	TT	SQ	MC
25	95	6.63176	6.63156	6.6307	6.6181	6.6317	6.63204
25	99.5	3.35542	3.35558	3.3552	3.3122	3.3564	3.35584
25	99.9	3.00848	3.00887	3.0095	2.9626	3.0098	3.00918
125	95	6.16797	6.16864	6.1678	6.1692	6.1687	6.16879
125	99.5	1.96143	1.96130	1.9617	1.9624	1.9628	1.96142
125	99.9	1.51098	1.51068	1.5138	1.5116	1.5123	1.5105

options, and actual barrier option values computed with these formulas hardly exists, partly because any computation using these formulas is still quite computer intensive. The scarcity of numerical option values in the scientific literature for discretely applied barrier options is essentially due to the lack of exact solutions for such options. We have thus listed in Table 7 some numerical values for a number of knock-out option values that incorporate dividend ( $q$ ) and rebate ( $Rb$ ) payments. The fixed options parameters are  $S = 100$ ,  $T = 0.5$ ,  $K = 100$ ,  $\sigma = 0.20$ ,  $r = 0.10$ . The various knock-out option types considered are the down-and-out, the up-and-out, and the double knock-out barrier options. The barrier application is either continuous or discrete in time. Numbers within parentheses in the table are CPU times.

In Table 7 the values of  $q$  and  $Rb$  are generally chosen to display some of the effects of these parameters. For example if we denote by  $Cbar$  and  $Dbar$  the value of a given barrier option under continuous monitoring and discrete monitoring respectively, and by  $Van$  the value of the corresponding vanilla option with same parameters, in the absence of rebates we must have

$$Cbar \leq Dbar \leq Van \tag{5.2}$$

and the generally very slow convergence of a discretely monitored barrier option can be verified using the inequalities in (5.2), given that the absolute error in the computation of  $Dbar$  is at most the difference ( $Van - Cbar$ ), and this yields a better approximation of  $Dbar$ , the more ( $Van - Cbar$ ) is small. Equation (5.2) is no longer true when the option pays a rebate, and many such examples appear in the table. The table also confirms that no matter what the options' monitoring frequency, dividend payments tend to drag down the call option value.

As far as the computing times are concerned, Table 7 shows that the CPU times in seconds for all the three types of knock-out options considered and for the given parameters are almost all between 0 and 0.5 seconds under continuous monitoring and do not exceed 1.18 seconds in any case. The computing times under continuous monitoring are smaller for values very close to the barrier, as already observed in Table 3. As for discretely monitored options, the computing time to achieve a very high accuracy can reach five thousand seconds, partly because it would be time consuming to try to find out the minimum amount of CPU time required in such

TABLE 7. Various HOBIS option values for continuously monitored and discretely monitored knock-out calls that incorporate rebate and dividend payments. The fixed parameters are  $S = 100, T = 0.5, K = 100, \sigma = 0.20, r = 0.10$ . For discrete monitoring the number of monitoring periods is 25 and the mesh size used is  $4000 \times 6000$ . Numbers within parentheses are CPU times.

$B_l$	$B_u$	q	Rb	Continuous	Discrete
Down - and - Out					
90	-	0.05	3	7.491 (0.42)	7.493
90	-	0.05	1.125	6.719 (0.55)	6.841
99.9	-	0.05	3	3.106 (0.04)	4.924
99.9	-	0	0	0.165 (0.03)	3.009
Up - and -Out					
-	110	0.20	0	0.225 (1.18)	0.344
-	110	0.02	0	0.299 (1.15)	0.470
-	100.1	0.0	0.01	0.009 (0.02)	0.009
-	100.1	0.0	3	2.987 (0.04)	2.735
Double Knock - Out					
95	125	0	0	2.033 (0.240)	3.008
95	125	0.04	6.66	7.057 (0.30)	7.256
75	185	0.045	0	6.863 (0.30)	6.864
80	120	0.04	0	2.196 (0.4)	2.654

case of very slow convergence to achieve a given level of accuracy. We have however noted that the computation of the discretely monitored double knock-out option with  $q = 0.045$  in the table gives the indicated value of 6.864 in only 4.20 seconds which turns out to be the limiting value, and this is truly a record CPU time for the computation of a discretely applied barrier option.

All of our nonuniform grid implementations as described in Section 4 did not yield any faster convergence or any better accuracy in the transformed  $(x, \tau)$  - coordinates. As in Section 4, denote by  $x_j$  the  $j$ th grid point in the  $x$  - direction, and by  $h_j = x_{j+1} - x_j$  the  $j$ th grid increment, and similarly let  $S_j = Ke^{x_j}$  and  $h_j^*$  be the corresponding grid point and grid increment in the original  $S$ -coordinates. Then we readily see that

$$h_j^* = (e^{h_j} - 1) \cdot S_j,$$

showing that a uniform grid in the  $x$ -coordinates (corresponding to  $h_j = h = \text{constant}$ ) always yields a nonuniform grid in the original  $S$ -coordinates. Moreover, such a nonuniform grid is typically sufficiently refined, since  $h$  is assumed to be small and thus  $e^h - 1$  is close to zero. For instance, if  $h = 1/10^4$  and  $S_j = 50$ , then  $h_j^* = 0.00500025$ . This shows that the implementation of effective nonuniform grids is not straightforward under the combination of the coordinates transformation and the high-order accurate FDS. For all of our attempts of nonuniform grids

in the  $x$ - or  $\tau$ -coordinates, we achieved the best results only when the non uniformity parameter  $q_j = h_j/h_{j-1}$  was equal to 1, which corresponds to the uniform grids discussed in this section.

## 6. CONCLUSIONS

For the valuation of various barrier options, we have used in this paper a finite difference scheme which is fourth-order accurate in the space variable and second-order accurate in the time variable. This scheme has been shown to be much faster and accurate than all of the most common schemes, namely the Crank-Nicolson, the explicit, and the fully implicit schemes. We've also given an optimal determination of the boundary conditions, which is particularly relevant for single-barrier options, but also for discretely monitored double knock-out options. In this way, with a reasonable accuracy we have been able to value continuously monitored barrier options in a fraction of seconds and with a mere  $20 \times 20$  mesh.

The efficiency of the combined high-order scheme and optimal determination of boundary conditions was again demonstrated in the difficult problem of valuing discretely monitored barrier options. Indeed, a comparison of the option values obtained using the resulting scheme with those obtained using five other numerical methods shows not only a good agreement, but also that our values are much closer to the sole method based on an analytical solution for discretely sampled barrier options. Our optimal determination of boundary conditions naturally has several applications, and could be used amongst others to classify double barrier options into simpler types of options.

## REFERENCES

- [1] V. Andreev, A. Popov, Richardson's method to construct high-order accurate adaptive grids, *Computational Mathematics and Modeling* 10 (1999) 227–238.
- [2] J. Barraquand, D. Martineau, Numerical valuation of high dimensional multivariate american securities, *Journal of Financial and Quantitative analysis* 30 (1995) 383–405.
- [3] M. Bertoli, M. Bianchetti, Monte carlo simulation of discrete barrier options, internal report, Financial Engineering - Derivatives Modelling, Caboto SIM S.p.a., Banca Intesa Group, Milan, Italy (2003).
- [4] P. Boyle, Y. Tian, An explicit finite difference approach to the pricing of barrier options, *Applied Mathematical Finance* 5 (1998) 17–43.
- [5] M. Broadie, P. Glasserman, S. Kou, A continuity correction for barrier options, *Math. Finance* 7 (1997) 325–349.
- [6] M. Broadie, J. Detemple, American capped call options on dividend-paying assets, *Review of Financial Studies* 8 (1995) 161–192.
- [7] P. Carr, Two extensions to barrier option valuation, *Applied Mathematical Finance* 2 (1995) 173–209.
- [8] T. Cheuk, T. Vorst, Complex barrier options, *Journal of Derivatives* 4 (1996) 8–22.
- [9] N. Clarke, K. Parrott, Multigrid for american option pricing with stochastic volatility, *Applied Mathematical Finance* 6 (1999) 177–195.
- [10] J. Duan, E. Dudley, G. Gauthier, J. Simonato, Pricing discretely monitored barrier options by a markov chain, *J. Derivatives* 10 (2003) 9–32.
- [11] B. Durrleman, M. Fournie, A. Jungel, High order finite difference schemes for a nonlinear black-scholes equation, *International Journal of Theoretical and Applied Finance* 6 (2003) 767–789.
- [12] G. Fusai, I. Abrahams, C. Sgarra, An exact analytical solution for barrier options, *Finance Stochast.* 10 (2006) 1–26.
- [13] G. Fusai, M. Recchioni, Numerical valuation of discrete barrier options, *J. Econ. Dynamics Control*. In press. (2006).
- [14] B. Gao, J. Huang, M. Subrahmanyam, The valuation of american barrier options using the decomposition technique, *Journal of Economic Dynamics and Control* 24 (2000) 1783–1827.

- [15] H. Geman, M. Yor, Pricing and hedging double-barrier options: A probabilistics approach, *Mathematical Finance* 6 (1996) 365–378.
- [16] E. Haug, Closed form valuation of american barrier options, *International Journal of Theoretical and Applied Finance* 4 (2001) 355–359.
- [17] S. Heston, A closed-form solution for options with stochastic volatility with applications to bond and currency options, *Rev. Financial stud.* 6 (1993) 327–343.
- [18] P. Heynen, H. Kat, Discrete partial barrier options with a moving barrier, *Journal of Financial Engineering* 5 (1996) 199–209.
- [19] H. Hsu, Surprised parties, *RISK* 10 (1997) 27–29.
- [20] S. Ikonen, J. Toivanen, Efficient numerical methods for pricing american options under stochastic volatility, reports of the department of mathematical information technology, Series B. Scientific Computing, No B12 (2005).
- [21] N. Kunitomo, M. Ikeda, Pricing options with curved boundaries, *Mathematical Finance* 2 (1992) 275–298.
- [22] A. Mayo, High-order accurate implicit finite difference method for evaluating american options, *The European Journal of Finance* 10 (2004) 212–237.
- [23] R. Merton, Theory of rational option pricing, *Journal of Economics and Management Science* 4 (1973) 141–183.
- [24] K. Morton, D. Mayers, *Numerical solution of partial differential equations*, 1st ed., Cambridge University Press, Cambridge, 2005.
- [25] A. Pelsser, Pricing double barrier options using laplace transforms, *Finance Stochast* 4 (2000) 95–104.
- [26] D. Rich, The valuation and behavior of the black-scholes options subject to intertemporal default risk, *Review of Derivatives Research* 1 (1996) 25–59.
- [27] M. Ross, *An introduction to Mathematical Finance*, Cambridge University Press, Cambridge, 1999.
- [28] M. Rubinstein, E. Reiner, Breaking down the barriers, *RISK* 4 (1991) 28–35.
- [29] J. Sidenius, Double barrier options: Valuation by path counting, *J. Computat. Finance* 1 (1998) 63–79.
- [30] R. Zvan, K. Vetzal, P. Forsyth, Pde methods for pricing barrier options, *Journal of Economic Dynamic & Control* 24 (2000) 1563–1590.

DEPARTMENT OF PHYSICS, UNIV. OF WESTERN CAPE, PRIVATE BAG X17, BELLVILLE 7535, SOUTH AFRICA.

*E-mail address:* `jndogmo@uwc.ac.za`

NBN, UNIV. OF WESTERN CAPE, PRIVATE BAG X17, BELLVILLE 7535, SOUTH AFRICA.

*E-mail address:* `ntwiga@nbn.ac.za`